

Ref. # JP 8611432

NAG 1-286
RECEIVED
LIBRARY

1988 APR 15 A 8:10

AIAA/TIS

7N-25-C12

270868

158

Absorption Cross Sections and Kinetic Considerations
of the IO species as Determined by
Laser Flash Photolysis/Laser-Absorption Spectroscopy

R.E. Stickel, A.J. Hynes, J.D. Bradshaw,
W.L. Chameides and D.D. Davis*

School of Geophysical Sciences
Georgia Institute of Technology
Atlanta, GA 30332

(NASA-CR-186430) ABSORPTION CROSS SECTIONS
AND KINETIC CONSIDERATIONS OF THE IO SPECIES
AS DETERMINED BY LASER FLASH
PHOTOLYSIS/LASER-ABSORPTION SPECTROSCOPY
(Georgia Inst. of Tech.) 15 p

N90-70705

Unclass

00/25 0270868

In Press
J. Phys. Chem.

Abstract

Reported are independent measurements of the absorption cross section of the IO radical for the $A^2\Pi - X^2\Pi$ band system. A value of $(3.1 \pm 0.6) \times 10^{-17} \text{ cm}^2$ was observed for the (4,0) bandhead in good agreement with an earlier investigation. Results are also reported for the (5,0), (3,0), (2,0), and (1,0) bands over the wavelength range of 410 to 470 nm. However, no measurable ($< 2 \times 10^{-18} \text{ cm}^2$) absorption was found for the (0,0) band. The atmospheric photodissociation rate constant, J_{IO} , for solar zenith angles of 0° to 40° was calculated to have a value of $(0.06 \pm 0.01) \text{ sec}^{-1}$. This value is a factor of five lower than previous estimates. Finally, the rate coefficient for the reaction $\text{IO} + \text{IO} \rightarrow \text{products}$ (3) has been measured at 760 torr N_2 and 300°K . The measured effective bimolecular rate constant was found to be $(6 \pm 2) \times 10^{-11} \text{ cm}^3 \cdot \text{molec}^{-1} \cdot \text{sec}^{-1}$, in good agreement with recent results by Sander (1986).

Introduction

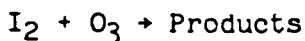
The role of iodine in tropospheric photochemistry has been the subject of speculation for several years.^(1,2,3) It has been proposed, for example, that methyl iodide as well as iodine in other chemical forms from marine sources or nuclear reactors can be photolyzed in the atmosphere to produce atomic iodine. It is further postulated that in the natural troposphere atomic iodine may participate in free radical driven chemical cycles that alter tropospheric levels of ozone, H_xO_y , and NO_x species³. Concerning the possible accidental release from nuclear reactors, the question posed is that concerning the atmospheric lifetime of radioactive iodine, and hence, its dispersal over large geographical areas via atmospheric transport processes.

The IO molecule has been identified as one of the key intermediates in the atmospheric iodine cycle (3,7,8); thus, both its photolytic and gas kinetic lifetime are in need of careful evaluation. The solar photolysis of IO occurs primarily via the $A^2\Pi + X^2\Pi$ band system in the 417 -470 nm spectral range. This system was discovered⁽⁴⁾ and, analyzed^(5,6) previous to 1961. However, no absolute photoabsorption cross section data were available until a low resolution spectrum was published in 1983⁽⁷⁾. Subsequently, the latter result has been substantially revised (8). The present work includes an independent measurement, at higher resolution, that confirms the original study by Cox and Coker⁷ while differing somewhat in the relative band intensities, particularly in regards to the (0,0) transition. The rotationally resolved (2,0) band spectrum presented here also supports the J-dependent predissociation suggested by a recent laser-induced fluorescence measurement⁽⁹⁾.

Experimental

Iodine monoxide was photochemically generated in this study by the laser flash photolysis of ozone in the presence of iodine. The source mixture was prepared by mixing two flows of nitrogen carrier gas; one that had been passed through a trap containing reagent grade iodine crystals and the other that had

been doped with zero grade air and passed through a discharge-type ozone generator. The ozone and iodine concentrations were monitored via optical absorption at 254 nm ($\sigma = 1.13 \times 10^{-17} \text{ cm}^2$, ref. 10) and 500 nm ($\sigma = 2.19 \times 10^{-18} \text{ cm}^2$, ref. 11), respectively. As shown in Fig. 1, optical absorption measurements of IO were recorded using the output of a XeCl excimer pumped dye laser. The dye laser output bandwidth was approximately 0.01 nm (FWHM). The analysis beam was typically passed through the sample chamber 60 times using a White cell⁽¹⁵⁾ configuration; however, the actual number of passes was limited by films forming on the AR coated chamber windows, presumably due to thermal reactions of the type:



The photolysis laser consisted of a KrF excimer laser which produced 30 mJ per pulse at 248 nm in a 12 mm x 12 mm beam. For absolute cross section measurements, the beam was apertured to 10mm x 10mm. The spatial homogeneity of the beam was verified by scanning a pinhole aperture across the beam profile and by inspecting burn patterns on photosensitive paper. Spatial variations were 10% or less. The photolysis energy was measured by a calibrated thermopile (Sciencetech) that was positioned immediately behind the sample cell. These raw measurements were then corrected for Fresnel losses using the measured transmissivity of the cell. Absorption of the photolysis beam by the sample gas was found to be negligible.

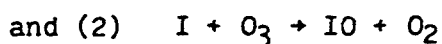
The total path length of the analysis beam through the photo active region of the sample chamber was defined by the product of the 10mm width photolysis beam and the number of passes through the chamber as determined both by direct count and by measurement of the time delay between input and output pulses. The validity of the latter approach was further confirmed by absorption measurements of NO_2 produced from the photolysis of HNO_3 .

For relative cross section measurements the 10mm x 10mm aperture was removed and the thermopile was replaced by a mirror which reversed the

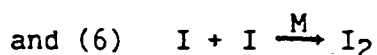
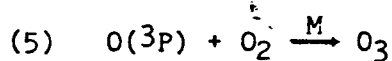
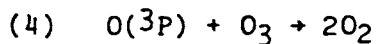
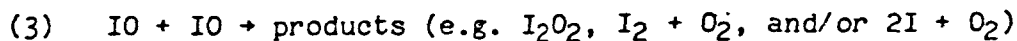
photolysis beam for a second pass through the sample, roughly doubling the IO concentrations. Stability of the [IO] was verified by frequent checks of the reference wavelength at 427 nm.

The pre-photolysis concentrations of I_2 and O_3 were varied over the range of 2.8 to 11×10^{14} molec. cm^{-3} and 1.7 to 4.3×10^{14} molec. cm^{-3} , respectively. In all cases the ozone level was near 1% of the oxygen level and the total pressure was ~ 760 Torr. The initial O atom concentration was computed as the product of the photolysis photon flux and an ozone absorption cross section (10) of 1.0×10^{-18} $cm^2 \cdot molec^{-1}$. The range of initial [O] observed was 2.7 to 4.5×10^{13} cm^{-3} with a single photolysis pass and roughly double that with two photolysis passes. Note that under our experimental conditions the primary process

$O_3 + h\nu \xrightarrow{\lambda=248 \text{ nm}} O(^1D) + O_2$ results in the production of $O(^3P)$ within nano-seconds of the photoflash due to the rapid quenching by nitrogen. Thus, the formation of IO involved the reactions:



Other potentially important reactions in this system include:



Results and Discussion

The rate equations resulting from reactions (1) through (6) were integrated numerically using a piecewise linear approximation⁽¹²⁾ to determine the concentration of IO in time. The rate coefficients used in this analysis were $k_1 = 1.38 \times 10^{-10}$ (13), $k_2 = 9.6 \times 10^{-13}$ (8), $K_3 = 6 \times 10^{-11}$, $k_4 = 8.9 \times 10^{-15}$ (14), $K_5 = 1.5 \times 10^{-14}$ (14) and $K_6 = 9.3 \times 10^{-13}$ (3). All k values are expressed here in $\text{cm}^3 \cdot \text{molec}^{-1} \cdot \text{s}^{-1}$. The uppercase K's represent bimolecular equivalent k's using a third body N_2 concentration of $2.5 \times 10^{19} \text{ molec} \cdot \text{cm}^{-3}$; however, K_3 represents the effective bimolecular K value, at one atmosphere pressure of N_2 , that encompasses the three different product channels as shown in equation (1). The value used here for K_3 is based on curve fitting the observed temporal variation in the IO absorption with model curves using several different values of K_3 . An example of such a comparison is illustrated in Fig. 2. For this experiment the initial I_2 and O concentrations were 6.2×10^{14} and $3.4 \times 10^{13} \text{ molec} \cdot \text{cm}^{-3}$ respectively. Each experimental point is an average of 15 individual absorbance measurements, each involving one photolysis pulse and two analysis/probe pulses. Although some of the values are negative none of them is more than one standard deviation below zero. The four smooth curves represent model results with K_3 values of 2, 4, 8 and $16 (\times 10^{-11} \text{ cm}^3 \cdot \text{molec}^{-1} \cdot \text{s}^{-1})$, respectively, from top to bottom.

From Fig. 2, two important findings are apparent. Firstly, with a factor of 8 change in K_3 , the peak [IO] concentration varies from 79% to 95% of the initial [O]. The cross section values computed from these data are thus largely insensitive to errors in K_3 . Secondly, at a total pressure of one atmosphere the value of K_3 of $\sim 2 \times 10^{-10} \text{ cm}^3 \cdot \text{molec}^{-1} \cdot \text{sec}^{-1}$, published in earlier works^(7,8), is clearly inconsistent with the observations of this work. The best fit to the current data from 7 experiments involving a range of [O] and $[\text{I}_2]$ levels indicates a K_3 value of $(6 \pm 2) \times 10^{-11} \text{ cm}^3 \cdot \text{molec}^{-1} \cdot \text{sec}^{-1}$, in good agreement with the recent measurement by Sander²⁰.

Iodine monoxide cross sections as a function of wavelength were assembled by first measuring the (4,0) bandhead cross section and then scanning the remainder of the spectrum with frequent references to the (4,0) head. Fig. 3 shows a composite of this spectrum numerically smoothed to an effective resolution of 0.3 nm for comparison with a previously published spectrum⁷. The (4,0) band is virtually identical in both works, and the current value of $3.1 \pm 0.6 \times 10^{-17} \text{ cm}^2$ for the (4,0) band head also agrees very well with more recent results²⁰. The relative intensities of the other bands are somewhat different from those of ref.(7), but the most striking discrepancy is the absence of the (0,0) band in the present work. Taking the noise level in the present data as an upper bound yields a (0,0) bandhead cross section of $< 2 \times 10^{-18} \text{ cm}^2$ or roughly 20 times below the value observed here for the (2,0) head. A theoretical estimate of the Franck-Condon factors⁽¹⁶⁾ results in a predicted 9:1 ratio and a laser-induced fluorescence observation revealed the (0,0) band to be less than one tenth the (2,0) intensity⁽⁹⁾. However, interpretation of the latter result⁹ is complicated by the predissociation of the $A^2\Pi$ state. In fact, the apparent rotational temperature of 70°K exhibited by the fluorescence spectrum was ascribed to a rotational dependence in the predissociation. This hypothesis would seem to be confirmed by the high resolution (2,0) band spectrum shown here in Fig. 4 which compares favorably to the 300°K prediction of ref. 9. The fluorescence spectrum of the (0,0) band was observed to have a more normal 300°K distribution suggesting that the (2,0) band may lose more in intensity to predissociation than the (0,0) transition, making the (0,0) band relatively more prominent in fluorescence than in absorption. The latter argument would seem to be in agreement with the current result.

The (3,1) band has been included in Fig. 3 but the relative intensity can not be interpreted in a straightforward manner because of the transient character of the vibrationally excited ground state. This band was not included in our estimate of the solar photolysis rate. An absorption feature near 410

nm, consistent with the (6,0) band of IO, was observed but a positive identification was not possible. This new band was well below the (5,0) band in intensity and did not contribute substantially to the evaluation of the atmospheric photolysis rate.

The rate of IO photolysis in the troposphere has been estimated from the data of Fig. 3 and the calculated solar fluxes from Peterson¹⁹. The resulting J value is $0.06 \pm 0.01 \text{ s}^{-1}$ for solar zenith angles from 0° to 40° and declines to $0.04 \pm 0.01 \text{ s}^{-1}$ at 80° . This value differs sharply from the value of 0.3 reported by Cox and Coker⁷. Apparently there are two sources for this discrepancy. Firstly, the average cross section values of Table II in Cox and Coker's work seem to be inconsistent with the data they present in their Fig. 1 which displays the IO cross section vs. wavelength. Secondly, they observed a greater degree of absorption between the individual IO bands than was seen in the present work.

The impact of our reported values of K_3 and J_{IO} on the tropospheric photochemistry of iodine will be addressed in a subsequent publication. The authors note, however, that meaningful modelling evaluations of this system must deal with not only new values for $J_{(IO)}$ and K_3 but must also assess the atmospheric photochemical fate of other key iodine species such as I_2O_2 and HOI, as well as various possible gas kinetic processes involving these same species. At this time, information on both I_2O_2 and HOI appears to be very limited and new studies, relevant to natural atmospheric conditions, would seem to be needed.

Acknowledgements

The authors would like to thank S. Fischer for providing the computer program used to integrate the kinetic rate equations. We also acknowledge the support of this research by NSF Grant #ATM 8113237.

References

- 1) Moyers, J.L.; and R. A. Duce, J. Geophys. Res. 1972, 77, 5229.
- 2) Zafirliou, O.C., J. Geophys. Res., 1974, 79, 2730 .
- 3) Chameides, W.L.; and D. D. Davis, J. Geophys. Res., 1980, 85, 7383 .
- 4) Vaidya, W.M., Proc. Ind. Acad. Sci. 1937, 6A, 122.
- 5) Coleman, E.H.; A.G. Gaydon and W.M. Vaidya, Nature, 1948, 162, 108 .
- 6) Durie, R.A.; F. Legay and D.A. Ramsay, Can. J. Phys., 1960, 38, 444 .
- 7) Cox, R A.; and G.B. Coker, J. Phys. Chem., 1983, 87, 4478 .
- 8) Jenkin, M.E.; and R.A. Cox, J. Phys. Chem., 1985, 89, 192 .
- 9) Inoue, G.M.; Suzuki and N. Washida, J. Chem. Phys., 1983, 79, 4730 .
- 10) Griggs, M.J.; J. Chem. Phys., 1968, 49, 857 .
- 11) Tellinghuisen, J.; J. Chem. Phys., 1973, 58, 2821 .
- 12) Hesstvedt, E.O.; Hov and I.S.A. Isaksen, Int. J. Chem. Kinet., 1978, 10, 971
- 13) Ray, G.W.; and R.T. Watson, J. Phys. Chem., 1981, 85, 2955 .
- 14) JPL, Publication 81-3, "Chemical Kinetic and Photochemical Data for use in Stratospheric Modeling - Evaluation Number 4: NASA Panel for Data Evaluation", Jet Propulsion Laboratory, California Institute of Technology, Pasadena, CA, 1981.
- 15) White, J.U.; J. Opt. Soc. Am., 1942, 32, 285 .
- 16) Rao, M.L.P.; D.V.K. Rao and P.T. Rao, Phys. Lett., 1974, A50, 341 .
- 17) Moyers, J.L.; and R. A. Duce, J. Geophys. Res., 1972, 77, 5229 .
- 18) Zafirliou, O.C.J.; J. Geophys. Res., 1974, 79, 2730 .
- 19) Peterson, J.P.; EPA Report 600/4-76-025, U.S. EPA, Research Triangle Park, NC, 1976, "Calculated Actinic Fluxes (290-700 nm) for Air Pollution Photochemical Applications".
- 20) Sander, S.P.; J. Phys. Chem., 1986, 90, p. 2194 .

Fig 1

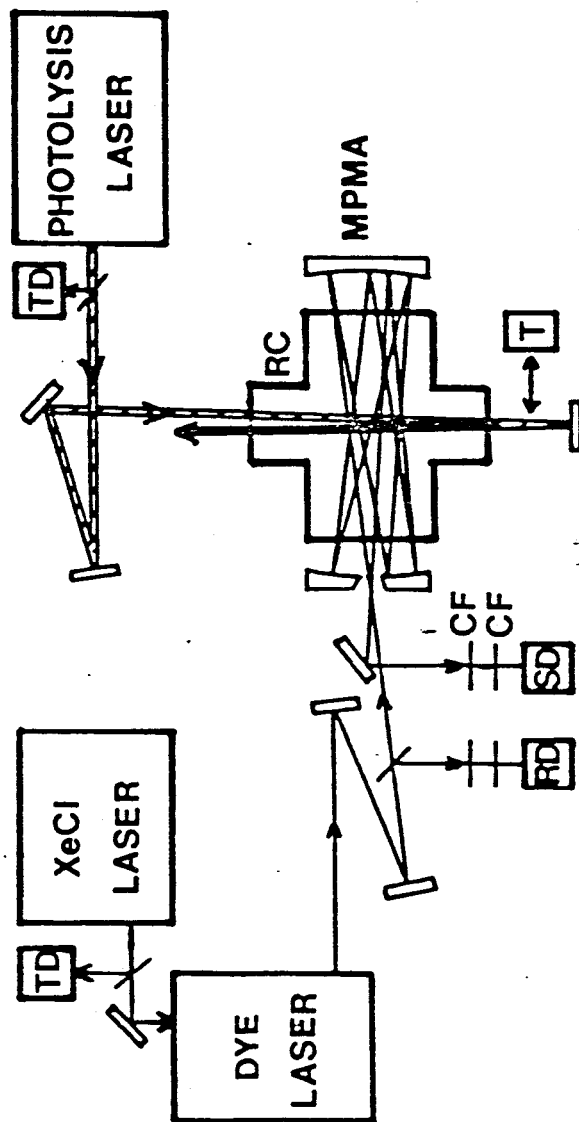
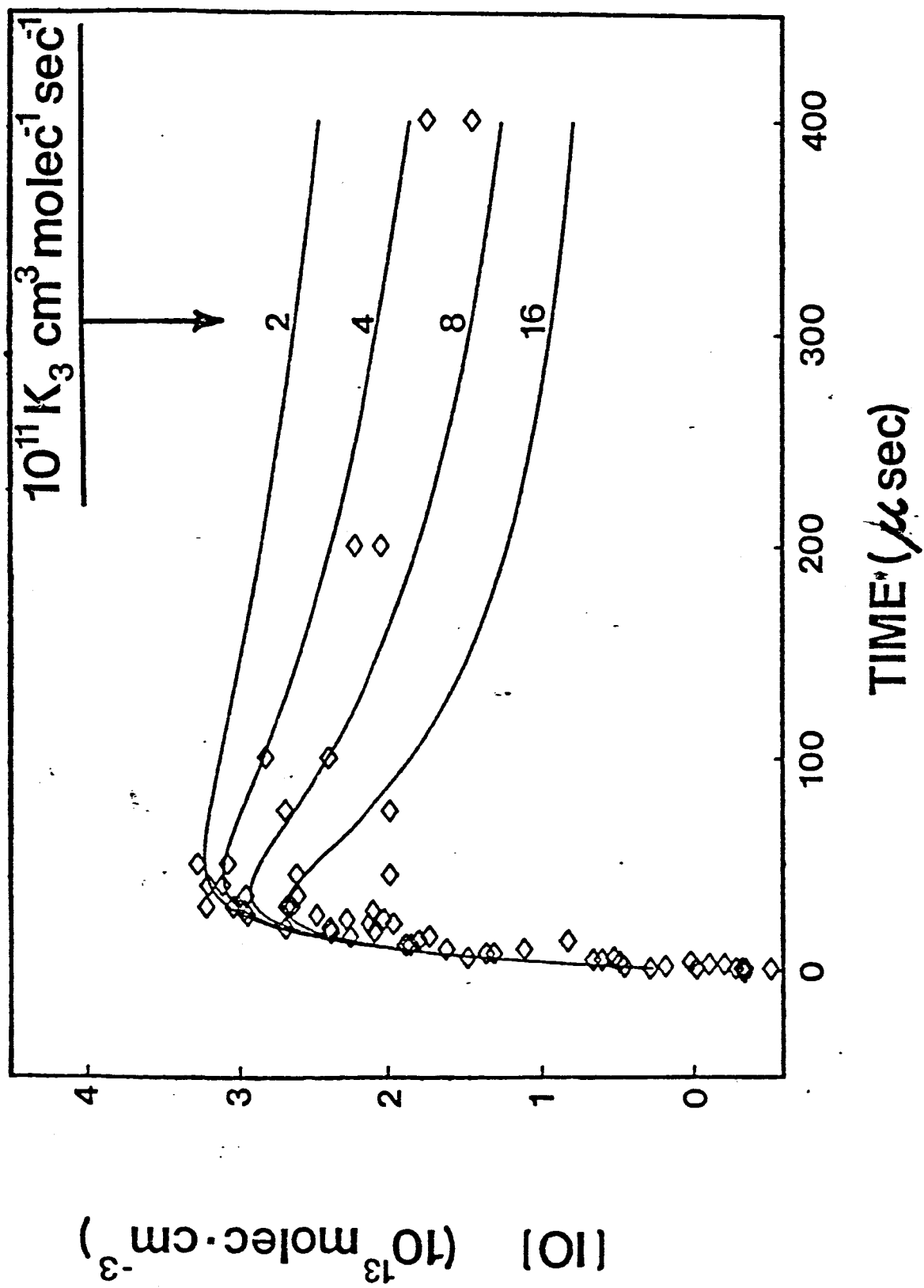


Fig 2



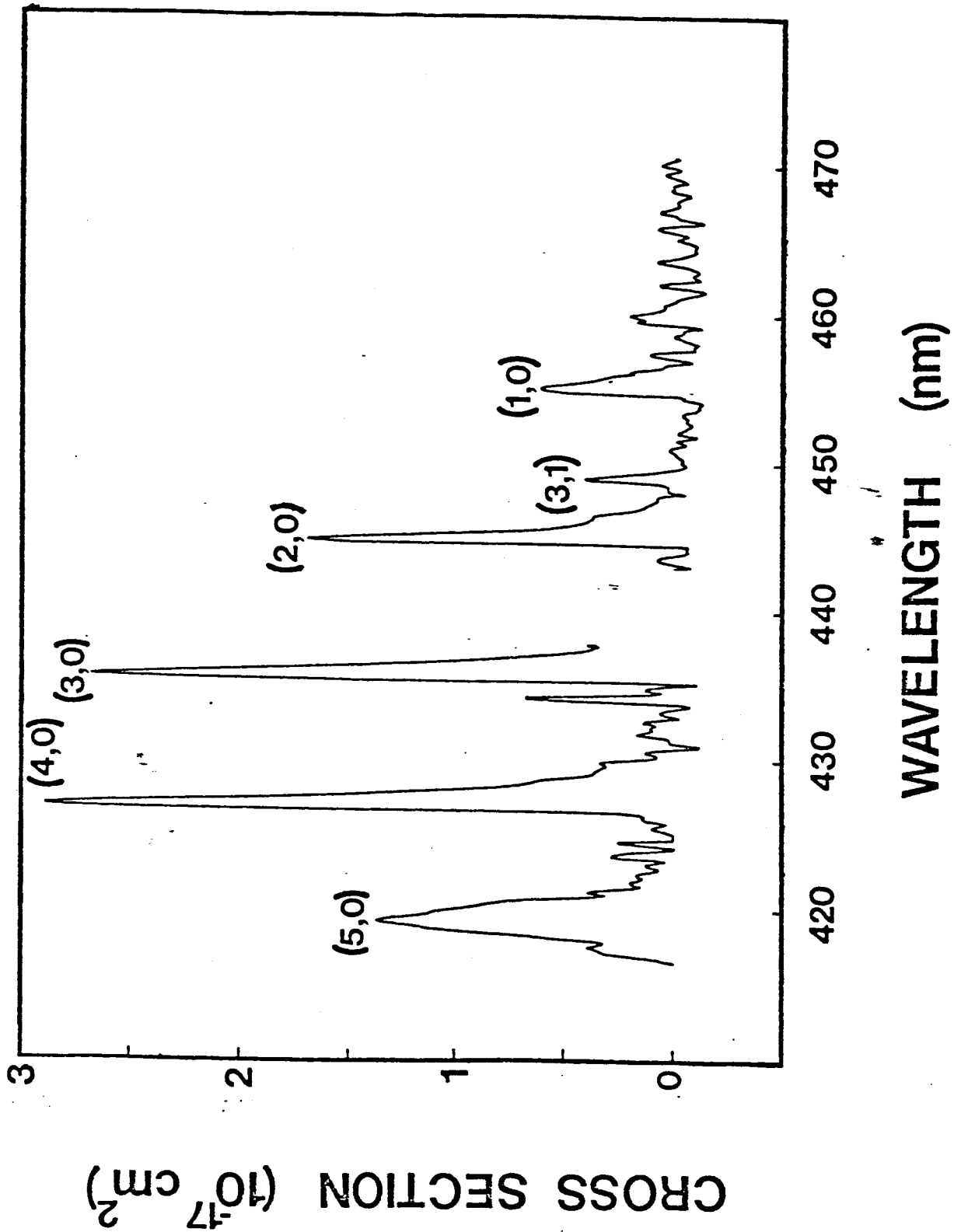


Fig 3

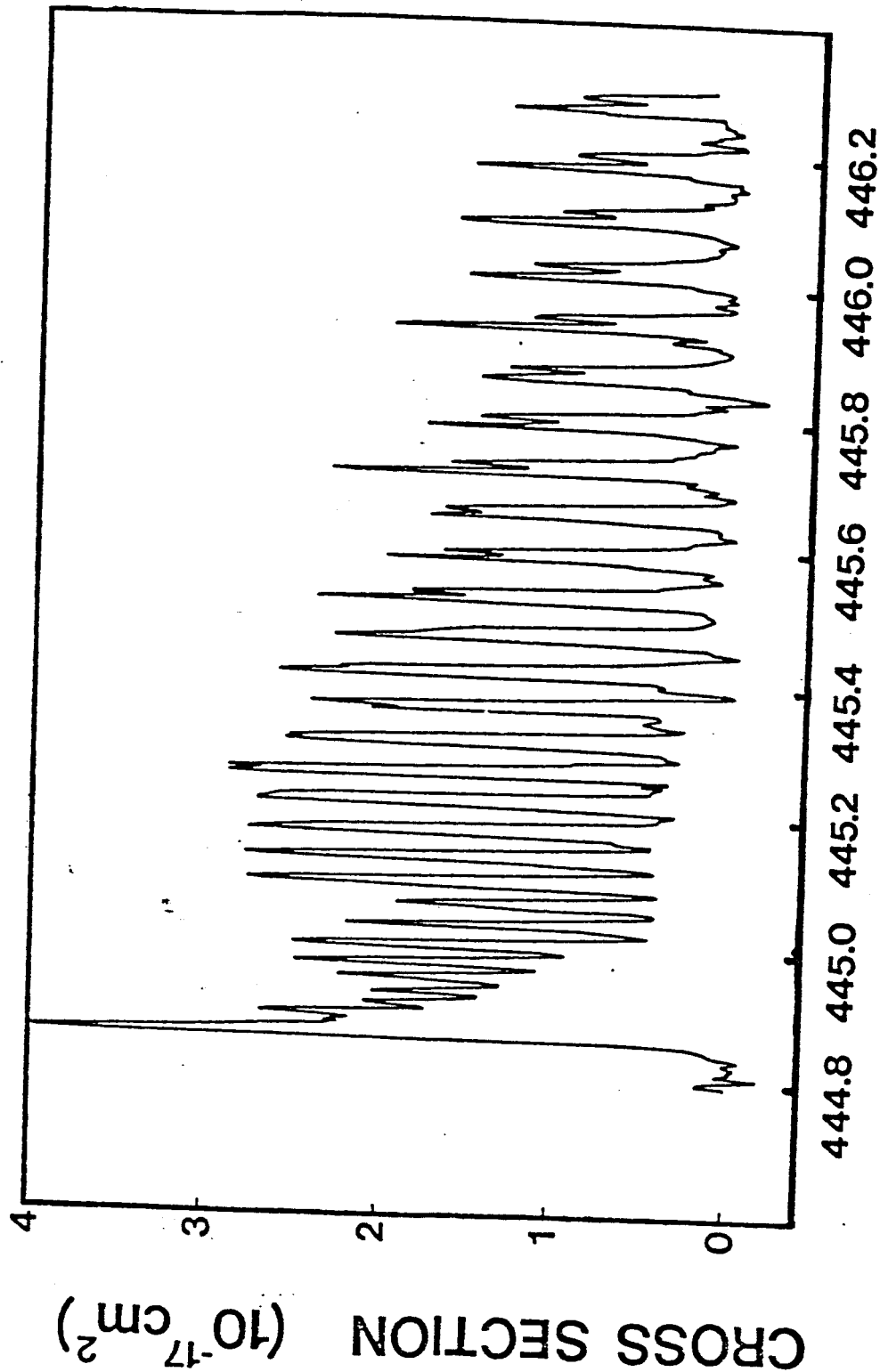


Figure Captions

- Fig. 1. Laser flash photolysis/laser-absorption spectroscopy hardware: RC - reaction cell, MPMA - multipass mirror assembly, RD - reference photodiode, SD - signal photodiode, TD - timing diode, T - thermopile, CF - color filters.
- Fig. 2. Profile of IO build-up and decay due to the reactions $O(^3P) + I_2$, $I + O_3$, and $IO + IO \rightarrow$ products.
- Fig. 3. Medium resolution plot of the IO absorption cross section versus wavelength for the (5,0), (4,0), (3,0), (2,0), (1,0), and (3,1) bands, resolution .3 nm.
- Fig. 4. High resolution plot of IO(2,0) band, .025 nm